Memoirs of the Graduate School of Engineering Kobe University
No. 1, pp. 42–47, 2009. doi:10.5047/gseku.e.2009.001

Effect of the Flow Rate of Water Dropping onto the Evaporator in an Absorption Chiller

Toru ISHIGAMI, Tsuyoshi KAMEDA, Hiroshi SUZUKI

Graduate School of Engineering, Department of Chemical Science and Engineering

(Received November 22, 2009; Accepted January 5, 2010; Online published January 18, 2010)

Keywords: Absorption Chiller, Liquid Film Model, Numerical Simulation, Water Drop Rate, Vapor Flow

Two-dimensional numerical study on the heat transfer characteristics and on a vapor flow in an absorption chiller has been performed to investigate the effect of water flow rate dropping onto the evaporator in an absorption chiller using the liquid film models previously developed. The flow rate was changed in three steps from 7.98 to 79.8 x 10^{-3} kg・m^{-1}・s^{-1} where the Reynolds number of liquid film ranged from 10 to 100. From the results, it was found that the evaporation and the heat transfer rates take peak values when the water dropped onto the evaporator reaches the bottom line of the evaporator cylinder bundle. The heat transfer was found to decrease severely with the flow rate after the peak mainly due to the thickening of the water liquid film. The pressure loss was also found to increase with the vapor flow velocity and it made the temperature difference between the saturation temperature and the heating temperature small. This was also partial cause on such severe decrease of the heat transfer rate after taking the peak value. From this, it was concluded that the optimum operating condition exists at the condition when the water just reaches the bottom line of the evaporator bundle.

1. Introduction

Related to the global warming and the ozone layer depression, environmentally-friendly air-conditioning systems are required. An absorption chiller attracts attention of many researchers working on saving energy because it can utilize exhausted heat and has no ozone depletion and no global warming potentials. However, it has some problems such as low coefficient of performance, long boot-time, the performance depression due to non-absorbable gas[1] and so on.

In order to improve these problems of the absorption chiller, many researchers reported the system analysis on the absorption systems. However, the heat transfer coefficients of the evaporator and of the absorber significantly depend on these cylinder alignments and the flow rate on the evaporator and the absorber. Thus, many experimental studies were required for the development of such an absorption chiller system.

Suzuki *et al.*[2], Suzuki and Sugiyama[3] and Ishigami *et al.*[4] developed liquid film models on the absorber and on the evaporator, respectively. These models do not depend on the cylinder alignment and flow rate in the range where the cylinder has no partial wet surface on each cylinder. With these, they reported reasonable heat transfer coefficient of the cylinder bundle in the evaporator and the absorber can be obtained for any cylinder alignment. Suzuki *et al.*[5] also applied the liquid film model to the numerical simulation of vapor flow and reported the non-absorbable gas behavior in the evaporator/absorber in an absorption chiller[6].

In this study, the effect of the flow rate of water dropping on the evaporator will be reported. High flow rate of water causes heat transfer decrease from cylinders because film thickness increases, and low flow rate causes dry out of cylinders. There exists the optimum condition for the system, but the performance of the system depends on the vapor flow causing pressure loss, which determines the temperature fields in the evaporator/absorber. It is difficult to measure the vapor flow field because the pressure is low around 900 Pa. Here, the vapor flow will be computed by using liquid film models as described. Then, the effect flow rate of water onto the top of the evaporator will be discussed.

2. Numerical Procedures

2.1 Computational domain and governing equations

In the present computations, only the flow and scholar fields of the water vapor were solved numerically and the thickness of liquid films falling along cylinders was not taken into consideration during solving the vapor flow. The liquid film was treated with the film theory only for determining the boundary condition on the cylinder surface as described in the next section.

The computational domain is shown in **Figure 1**, schematically. The evaporator with 4 x 20 of cylinders and the absorber with 4 x 24 were mounted in a rectangular computational domain with 0.912 x 0.580 m^2. The cylinder diameter, d [m], was 19 mm and the pitch between the cylinders, p [m], was 30 mm (p/d=1.63). The distance between the evaporator and the absorber was set at 300 mm. In order to calculate the flow and scholar fields around the cylinder, the multi-grid system[6] in which Cartesian coordinate system is used for main grid system covering all over the domain and cylindrical system for sub-grids assigned in a narrow region around each cylinder was applied as shown in **Figure 2**. Then, two kinds of equation sets of two-dimensional, time-dependent momentum, and energy, which correspond to respective coordinate systems, are used as reported by Suzuki *et al.*[7]. Bousinesq approximation was applied for buoyancy term caused by temperature. All properties included in the governing equations were assumed to be constant.

The finite difference equivalents of these governing equations were numerically solved. The central finite difference for diffusion terms, and the third-order upwind scheme, QUICK[8] for convection terms were respectively applied. Fully implicit form was used for time marching method. The pressure fields were calculated by SIMPLER[9] algorism.

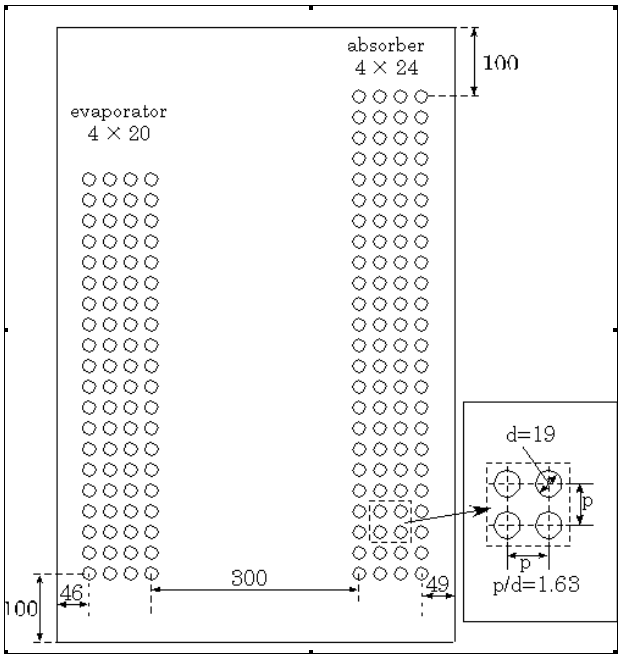

Fig. 1 Computational domain

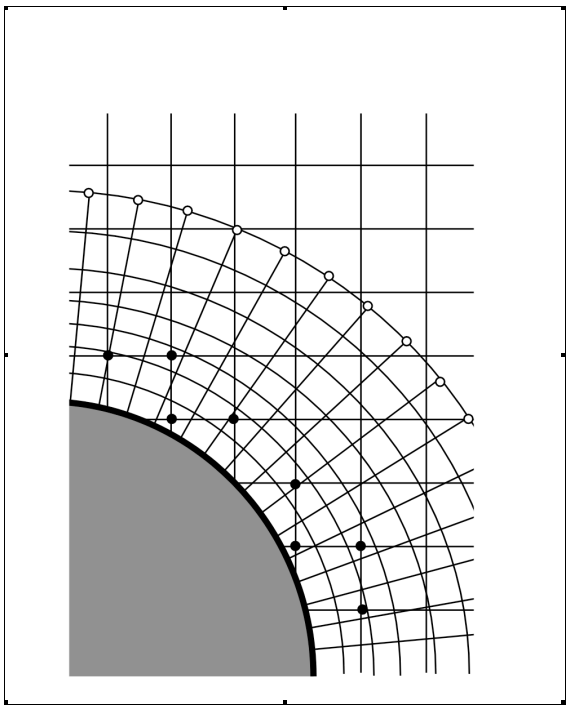

Fig. 2 Multi-grid system

2.2 Liquid film model

The boundary condition on the cylinder surface of the evaporator was determined with the water liquid film model developed by Ishigami *et al*[4]. On the other hand, the condition on the cylinder surface in the absorber was set with the LiBr solution liquid film model suggested by Suzuki *et al*[2]. As the initial condition, the vapor velocity was set at zero, while the liquid films were assumed to be fully developed without evaporation and absorption. The mass flow rate per unit length of water liquid film, G_0 [kg·m^{-1}·s^{-1}], dropped onto the top of the evaporator was changed in three steps from 7.98 to 79.8 x10^{-3} kg·m^{-1}·s^{-1}. In the present condition, the Reynolds number, *Re* [-] defined as the following equation is changed from 10 to 100.

$$Re = \frac{2G_0}{\mu_L} \qquad (1)$$

Here, μ_L [Pa·s] is the viscosity of water, respectively. In the present conditions, the liquid film can be assumed to be laminar.

Table 1. Computational Conditions

Chilled Water	
Inlet Temperature	12 °C
Flow rate	3,025 kg·h^{-1}
Cooling Water	
Inlet Temperature	32 °C
Flow Rate	3,025 kg·h^{-1}
Dense LiBr Solution	
Concentration	58.5 wt%
Flow rate	4.37x10^{-2} kg·m^{-1}·s^{-1}
Initial Pressure	918.6 Pa

The other conditions were tabulated in **Table 1**. In this study, the initial pressure in the computational domain was given but the final pressure was automatically determined at a certain value as taking the balance between the evaporation and the absorption when the flow field becomes steady. The value partially relates to the pressure loss of the vapor flow field as discussed later.

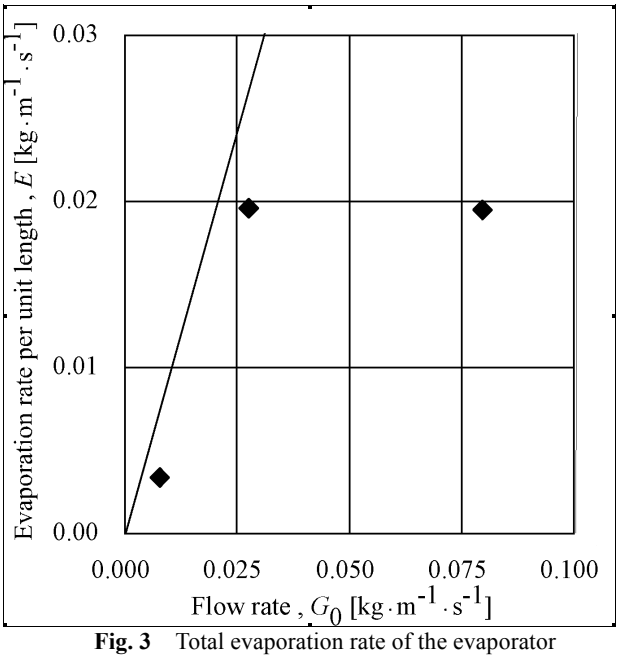

Fig. 3 Total evaporation rate of the evaporator

3. Results and Discussions

3.1 Evaporation and heat transfer characteristics

Figures 3 and **4** show the effect of the water flow rate per unit length onto the top of the evaporator bundle on the total evaporation rate per unit length, *E* [kg·m^{-1}·s^{-1}] and on the total heat transfer rate per unit length into the cylinder surface,

Q [W・m^{-1}]. In Figure 3, the values in the case when the mass dropped onto the bundle perfectly are evaporated are plotted in a solid line.

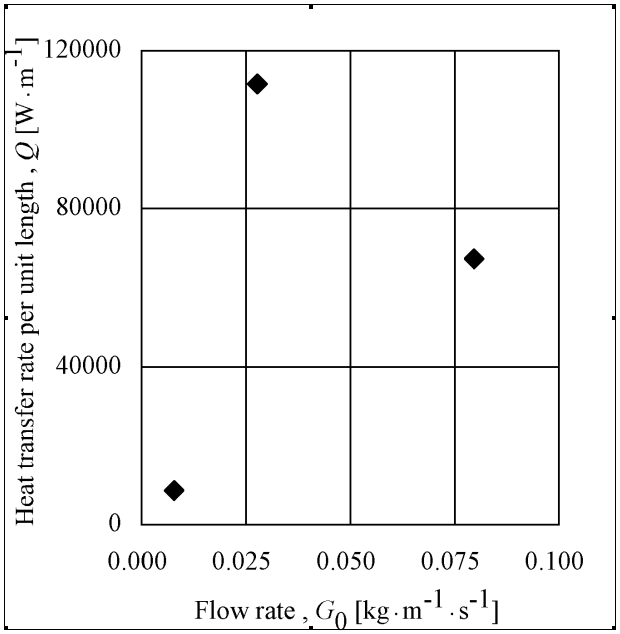

Fig. 4 Total heat transfer rate of the evaporator

From Figure 3, the evaporation is found to follow the perfect evaporation line until G_0 = 2.79x10^{-3} kg・m^{-1}・s^{-1}. However, the evaporation rate slightly decreases with the flow rate of water dropping onto the evaporator after it takes a peak value. It is also found that the heat transfer rate decreases after the peak.

When the water flow rate is small, water perfectly evaporates at a certain line of the evaporator bundle before it does not reach the bottom line. At this peak point, the water dropped onto the evaporator bundle just reaches the bottom cylinder line of the bundle and all cylinders are wetted. As the water flow rate increases after this peak, the liquid film thickness grows due to non-evaporated water. Then, heat transfer from the liquid film to the cylinder surface becomes small. Corresponding to this, the evaporation rate slightly becomes small with water flow rate.

The heat transfer rate decreases more severely compared with the evaporation rate after the peak. It is found that the heat transfer shows 40 % reduction of the peak value when G_0 = 7.98x10^{-2} kg・m^{-1}・s^{-1}, while the evaporation rate remains only 5% reduction. This heat transfer severely affects the performance of the absorption system. In the cases when the film thickness is small as the low flow rate cases, the temperature distributes linearly in the liquid film. When the film thickness becomes large, however, the heat from the cylinder is used only for heating the liquid film. Thus, the bulk temperature increases downward and the temperature gradient on the cylinder surface becomes small, while the temperature gradient becomes high on the film surface, which aids evaporation from the film surface. This temperature distribution causes the reduction rate difference between the heat transfer and the evaporation rates.

Figures 5 and **6** show the line average evaporation rate, E_i [kg・m^{-1}・s^{-1}] and the line average heat transfer rate, Q_i [W・m^{-1}] for each line of the evaporator. The line number, i[-] is numbered from the top (the 1st line), to the bottom (the 20th line), of the evaporator bundle.

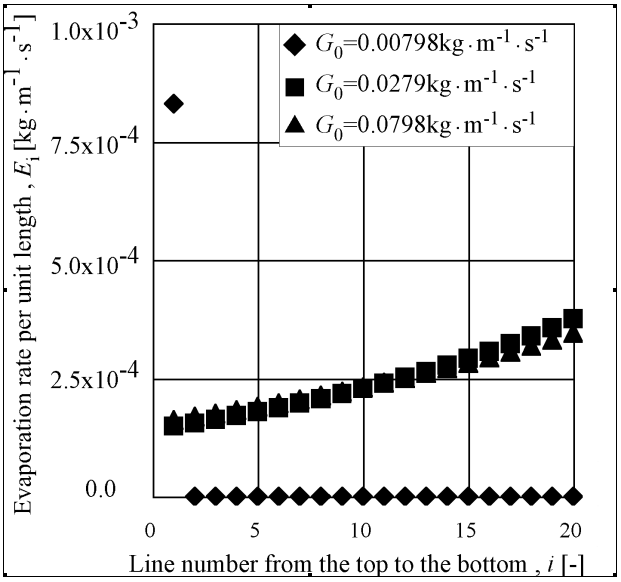

Fig. 5 Evaporation rate on each line of the evaporator

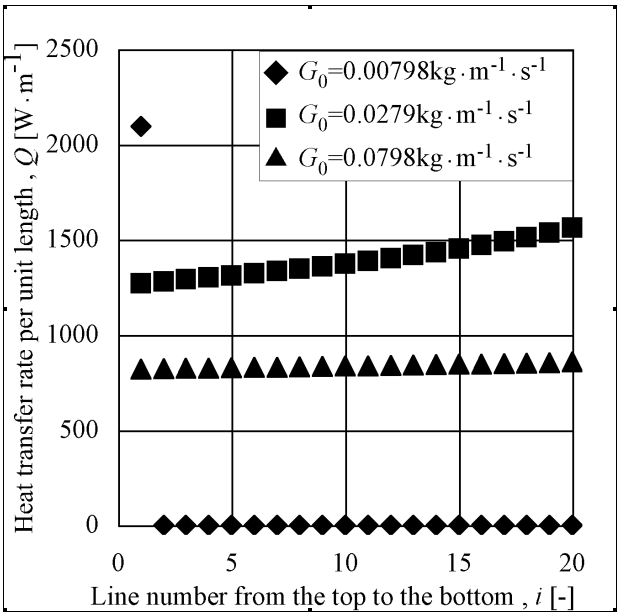

Fig. 6 Heat transfer rate on each line of the evaporator

In the case when G_0 = 7.98x10^{-3} kg・m^{-1}・s^{-1}, the water perfectly evaporates at the 1st line, and then the heat transfer becomes zero at lower cylinders. This dry-out causes the heat transfer reduction when the flow rate is small. When the flow rate becomes larger than 2.79x10^{-2} kg・m^{-1}・s^{-1}, the water reaches the bottom line and evaporates from each cylinder. It is found that the evaporation rate and the heat transfer rate increases downward, because the film thickness becomes smaller due to the evaporation. Compared with the results in the case when G_0 = 2.79x10^{-3} kg・m^{-1}・s^{-1}, the increases ratio of the evaporation rate in the case when G_0 = 7.98x10^{-2} kg・m^{-1}・s^{-1} becomes small. This increase tendency is also found in the behavior of the heat transfer rate. However, the heat transfer rate in the case when G_0 = 7.98x10^{-2} kg・m^{-1}・s^{-1} shows lower values at each line than that

in the case when G_0 = 2.79x10^{-3} kg・m^{-1}・s^{-1} and it becomes almost a half value at the bottom line of the bundle.

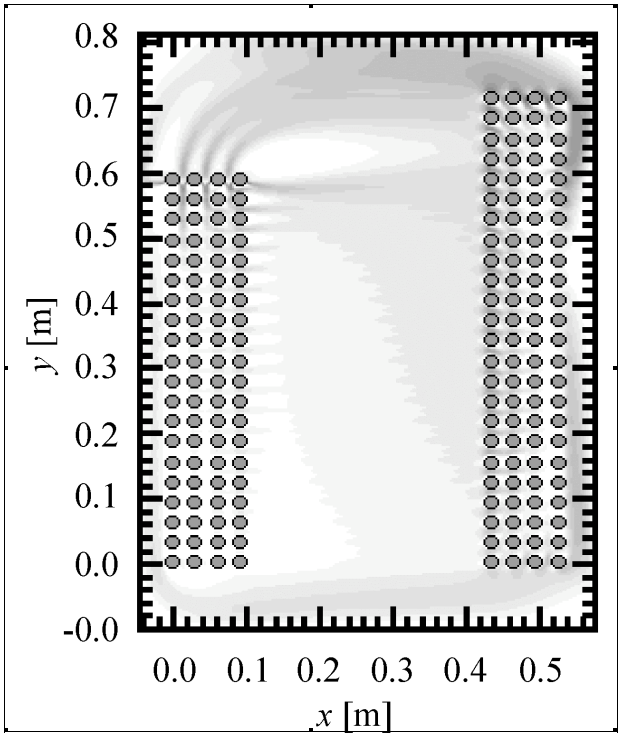

Fig. 7 Velocity contour when G_0 = 7.98x10^{-3} kg・m^{-1}・s^{-1}

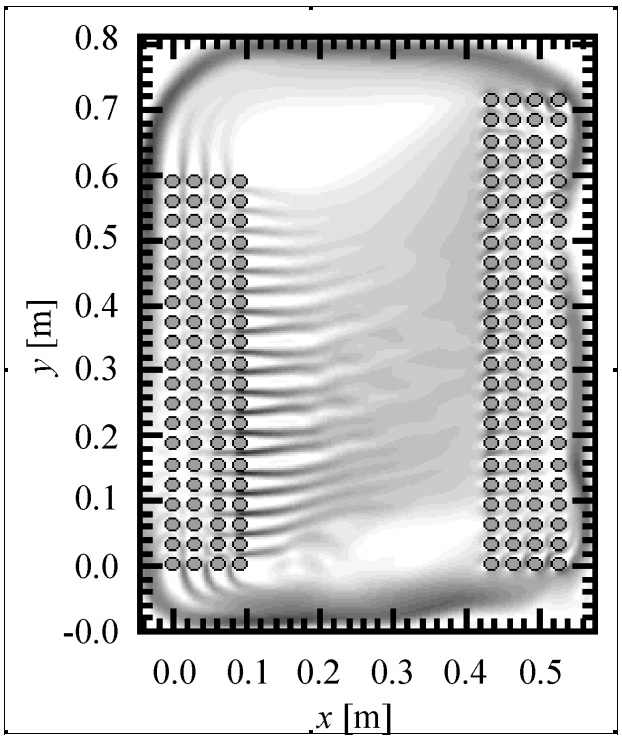

Fig. 8 Velocity contour when G_0 = 2.79x10^{-2} kg・m^{-1}・s^{-1}

Additionally, it is found that the heat transfer rate in the case when the film thickness becomes the largest takes almost a constant value from the top to the bottom line of cylinders. This corresponds to the fact that the film thickness takes almost the same value on each cylinder as the evaporation effect on the film thickness decrease ratio becomes small.

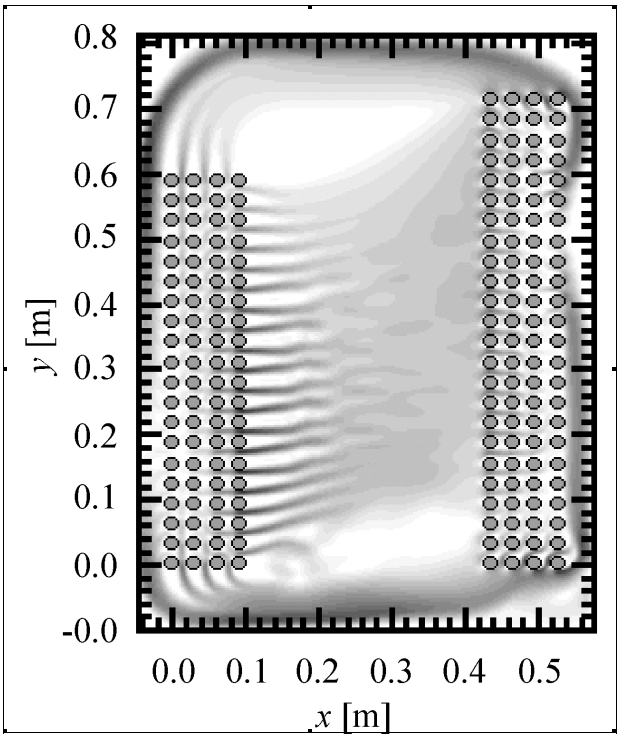

Fig. 9 Velocity contour when G_0 = 7.98x10^{-2} kg・m^{-1}・s^{-1}

3.2 Vapor flow characteristics

Figures 7-9 show the velocity contours of vapor in the evaporator-absorber for the cases when G_0 = 7.98x10^{-3}, 2.79x10^{-2} and 7.98×10^{-2} kg・m^{-1}・s^{-1}, respectively. In the figures, the color becomes darker as the absolute values of the velocity increases. The absolute values of velocity was normalized by the maximum value observed in the case when G_0 = 7.98x10^{-3}. In the figure, the left cylinder bundle is the evaporator and the right one is the absorber.

From Fig. 7, it is found that the high velocity region exists only the upper region of the evaporator/absorber. This is because the evaporation occurs only from the top cylinder film surface. On the other hand, the high velocity region exists not only in the upper region but also in the lower region and the middle region between evaporator and the absorber in the cases when the flow rate is larger than 2.79x10^{-2} kg・m^{-1}・s^{-1}as shown in Figs 8 and 9. As reported by Suzuki *et al*., the low velocity region is also observed to form between these high velocity regions. Thus, the flow field has high and low velocity regions. This causes high local pressure loss and it affects the heat transfer characteristics.

Figure 10 shows the average pressure, P_{ave} [Pa] for each flow rate. From this, the pressure increases slightly with the flow rate dropped on the evaporator bundle. This pressure increase is considered to correspond to the flow pressure loss and makes the saturation temperature, T_{sat} [^{o}C], at the average pressure higher as shown in **Figure 11**. In the present condition, the chilled water temperature is 12 ^{o}C. Then, this saturation temperature increase is found to affect the heat transfer characteristics of the evaporator. Thus, the vapor flow pressure loss is concluded to be a partial cause on

the heat transfer reduction after the peak condition. As shown in this study, the investigation of the flow field is very important for the design of the evaporator/absorber and for finding the optimum operating condition.

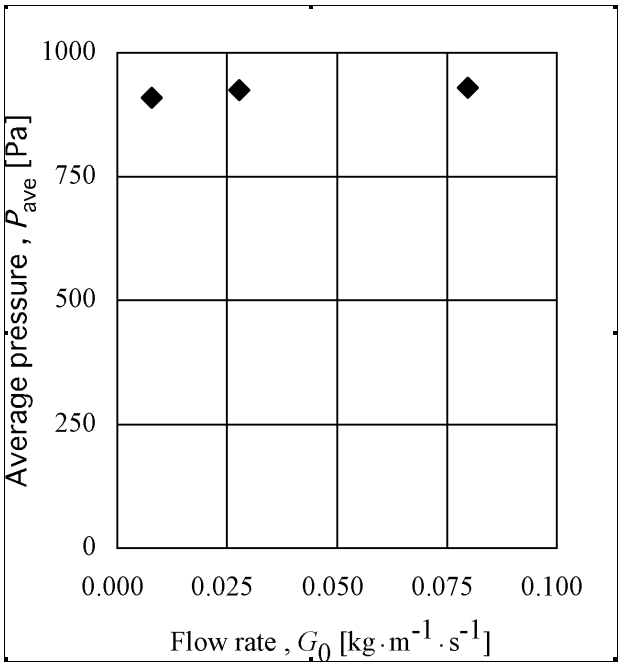

Fig. 10 Average pressure in the evaporator/absorber

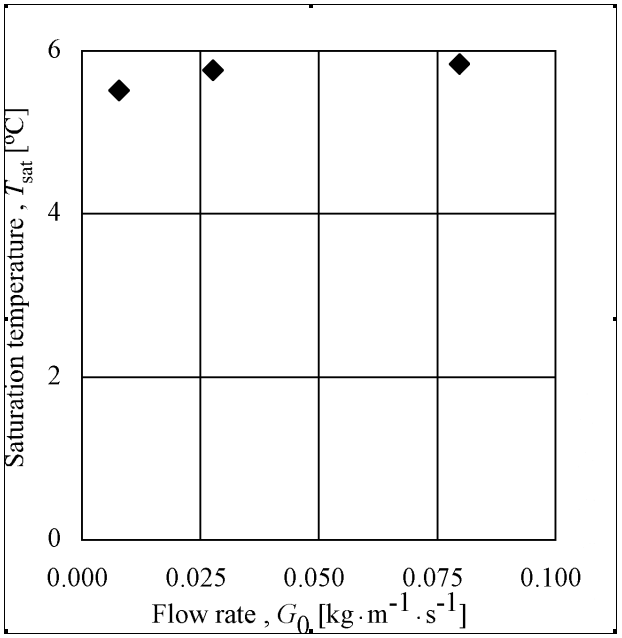

Fig. 11 Saturation temperature in the evaporator/absorber

4. Conclusions

Two-dimensional numerical study on the heat transfer characteristics and on a vapor flow in an absorption chiller has been performed to investigate the effect of water flow rate dropping onto the evaporator in an absorption chiller using the liquid film models previously developed. The flow rate was changed in three steps from 7.98 to 79.8 x 10^{-3} kg·m^{-1}·s^{-1} where the Reynolds number of liquid film ranged from 10 to 100. From the results, it was found that the evaporation and the heat transfer rates take peak values when the water dropped onto the evaporator reaches the bottom line of the evaporator cylinder bundle. The heat transfer was found to decrease severely with the flow rate after the peak mainly due to the thickening of the water liquid film. The pressure loss was also found to increase with the vapor flow velocity and it made the temperature difference between the saturation temperature and the heating temperature small. This was also partial cause on such severe decrease of the heat transfer rate after taking the peak value. From this, it was concluded that the optimum operating condition exists at the condition when the water just reaches the bottom line of the evaporator bundle.

Nomenclature

d	= cylinder diameter	[m]
E	= total evaporation rate	[kg·m^{-1}·s^{-1}]
E_i	= evaporation rate on i line	[kg·m^{-1}·s^{-1}]
G_0	= flow rate	[kg·m^{-1}·s^{-1}]
i	= line number	[-]
P_{ave}	= average pressure	[Pa]
p	= pitch between cylinders	[m]
Q	= total heat transfer rate	[W·m^{-1}]
Q_i	= heat transfer rate on i line	[W·m^{-1}]
Re	= Reynolds number	[-]
T_{sat}	= saturation temperature	[°C]
x	= horizontal coordinate	[m]
y	= vertical coordinate	[m]
μ_L	= water viscosity	[Pa·s]

Literature Cited

1) Yang, R. and T.-M. Jou; "Non-Absorbable Gas Effect on the Wavy Film Absorption Process", *Int. J. Heat Mass Transfer*, 41, 3657-3668 (1998)
2) Suzuki, H., T. Yamanaka, W. Nagamoto, T. Sugiyama; "Modeling of Liquid Film along Absorber Cylinders in an Absorption Chiller", *Trans. JSRAE*, 17, 213-221(2000), (in Japanese).
3) Suzuki, H. and T. Sugiyama; "Non-Absorbable Gas Diffusion Behavior in the Evaporator-Absorber in an Absorption Chiller", *Kagaku Kogaku Ronbunshu*, 27, 581-587 (2001), (in Japanese).
4) Ishigami, T, T. Kameda, H. Suzuki and Y. Komoda; "Development of a Liquid Film Model for the Evaporator in an Absorption Chiller", *Kagaku Kogaku Ronbunshu*, 35, 417-424 (2009), (in Japanese).
5) Suzuki, H., W. Nagamoto and T. Sugiyama; "Simulation on Vaper Flow in the ABsorber/Evaporator of an Absorption Chiller", *Trans. JSRAE*, 20, 325-331(2003) (in Japanese).
6) Suzuki, H., W. Nagamoto and T. Sugiyama; "Non-Absorbable Gas Behavior in the Absorber/Evaporator of an Absorption Chiller", *Trans. JSRAE*, 20, 333-340, (2003) (in Japanese).
7) Suzuki, H., Y. Iwasaki, K. Hara, Prabowo and Y. Kikuchi; "Combined Forced and Natural Convective Heat Transfer around a Cylinder in a Duct", *Proc. 10th Int. Sym. Transport Phenomena in Thermal Science & Process Eng,* 3, 895-900 (1997) Kyoto.
8) Leonard, B.P.; "A Stable and Accurate Convective Modeling Procedure Based on Quadratic Upstream

Interpolation", *Comput. Meth. Appl. Mech. Eng*.,19, 59-98(1979).
9) Patankar, S.V.; *Numerical Heat Transfer and Fluid Flow*, Hemisphere, (1980) Washington.